

Developing a New Algorithm to Detect Right Thumb Fingernail in Healthy Human

Aseel Thamer Ebrahem¹, Noor K. Younis¹, Azhar W. Talab¹, Zaid H. Al-Sawaff^{1,2}, Fatma Kandemirli³

¹Technical Engineering College, Northern Technical University (NTU)

²Central Research Lab, Northern Technical University (NTU)

Mosul, Iraq

aseelthamer@ntu.edu.iq

noorky@ntu.edu.iq

azhar.w@ntu.edu.iq

zaidalsawaff@ntu.edu.iq

³Faculty of Engineering and Architecture, Kastamonu University

Kastamonu, Turkey

fkandemirli@yahoo.com

Abstract—Due to significant challenges faced by traditional methods of personal identification like fingerprinting, eye scanning, and voice recognition, new techniques are needed. One such approach involves the use of human nail images for identification and access to personal identification programs and electronic patient files. A novel algorithm, which consists of three stages, has been proposed utilizing the HSV color space detection algorithm, grayscale contrast optimization algorithm, nail segmentation, and image smoothing with a Gaussian filter. This method reduces tested image data and preserves the primary image structure, and has the potential to surpass the accuracy of traditional methods, providing an additional layer of security in personal identification programs and electronic patient files. Nail image detection can be conducted remotely and accessed through standard cameras or smartphones, making it a more hygienic and convenient option than physical contact methods such as fingerprinting or eye scanning. Moreover, the use of nail images for personal identification has several other benefits, especially in situations where traditional methods are not feasible, such as in individuals with skin conditions that prevent fingerprinting. The success of the proposed algorithm in detecting nail images for personal identification has implications beyond individual security and can be applied in different fields, including healthcare and forensic science, to improve identification accuracy and prevent fraud. For example, the use of nail images could help prevent identity theft in healthcare settings, where sensitive information is stored and exchanged.

Keywords—Biometric authentication; Nail plate; Fingernails; Lunula; Image processing

I. INTRODUCTION

The most flexible and efficient way of identifying or authenticating individuals is through biometric identification systems [1,2]. One of the primary advantages of these systems is that the user does not need to remember or write down passwords or carry smart cards, leading to faster usage and reduced password management costs. Recently, researchers have been focusing on developing touchless acquisition systems to reduce the risk of attacks by fraudsters. These systems capture unique features of an individual without physical contact, such as joint structure, nails, or hand structure [3].

Anatomical studies of nails reveal that the nail plate is the only part that regenerates with the production of new cells, while the distance between nail grooves remains relatively constant throughout the nail's life. These grooves are highly distinctive and differ even between identical twins and the nails of the same hand [4]. As a result, this research relied on the nail bed as a primary method for measuring changes in biometrics.

Figure 1 displays the anatomy of the human fingernail.



Figure 1 illustrates the finger nail typical sample, with nail anatomy

A group of researchers has proposed the concept of transient biometrics as a current approach for identifying certain biometrics. The authors focused on established vital characteristics and used the nail as a case study, extracting images of fingernails using different texture features. However, results indicated that the photos were reliable for only one month due to changes in the tissue on which the samples were taken, making it suitable for measuring only transient vital activities [5]. Another study proposed an automated biometric authentication approach using fingernails based on the back view of the hand and three fingers of one hand. The nail plate was neglected, and the area called the nail bed was extracted

based on grayscale values. The proposed system gave less accurate validation results than systems that use a single surface of the nail [6]. A new system was proposed to recognize fingerprints without touching the device to the hand, relying on low-resolution cameras to take a picture of the user's hand. The system used the ROI technique to track the image of the hand and extract preset points of interest for the palm-based technique by applying the LBP to the gradient responses in the direction of printing. The experiments showed promising results, with the verification period not exceeding one second for each scan [7]. Another technique combined the features of nails and finger joints simultaneously, relying on an algorithm to extract ROI from joints and nails. The finger joint features were taken out using the MFCC technique, and nail characteristics were extracted from second-level wavelet decomposition. These parts were combined using feature-level fusion back-propagation neural network feeding. However, the system did not consider the nail plate and relied only on instantaneous images taken, leading to potential failure in the future [8]. The nail's unique property is that the average person's shape and size of the nail plate remain constant with age. The lunula, a white half-moon-shaped area found in the proximal ends of the nails, grows behind the edge of the proximal nail fold and can be considered a key to developing biometric authentication systems based on nails. This research proposes using the nail lunula to measure biometric

authentication applications, as it has advantages that differ from one person to another [9-15].

This paper is organized into four sections, with the first covering the introduction, the research problem, and literary reviews. The second section discusses the proposed system and how it works. The third section discusses the experimental results, and the fourth concludes the research, presenting final discussions and future visions for developing the research topic.

II. METHODOLOGY

DATA SET

In the current study, one hundred volunteers (fifty men and fifty women, with ten people of each sex between the ages of twenties to sixties) were selected, and no volunteers participated who have a history of injury or infection to their finger or toenail. We recorded details related to age, length of hands and fingers, and their proportion to body length to ensure that more information was collected in a standard position and an adequate assessment of the standard nail size.

In order to take the appropriate measurements, the previous studies were all taken into consideration, which included the best methods for measuring the length and width of the nail [16,17], where the width of the nail was defined as the farthest transverse distance between two points of the nail in the lateral groove. The length of the nail was defined as the furthest distance that can be measured between the tip of the finger and the groove resulting from the intersection of the nail fold as shown in Figure 2.

Table 2. Fingernails W/L ratio with the radius of transverse fingernails curvature for the age groups under investigation

Measurements	20	30	Age groups		
			40	50	60
Men					
Thumb W/L ratio	1.05±0.07	1.03±0.08	1.03±0.1	1.04±0.07	1.03±0.05
The radius of transverse thumb curvature (mm)	9.8±0.9	10.2±0.8	10.4±1.3	11.3±1.5g	11.3±1.4
Women					
Thumb W/L ratio	0.91±0.08	0.91±0.09	0.91±0.1	0.91±0.06	0.92±0.05
The radius of transverse fingernail curvature (mm)	9.3±0.9	9.3±0.7	9.6±0.8	9.9±0.8	10.1±0.6

Also, to assess nail curvature, we measured the radius of the circle whose curvature approaches the nail plate, as shown in Figure 3. After that, the ratio of the length of the nail to its width was measured, and all the results were recorded in order to arrive at the final shape of the standard nail.

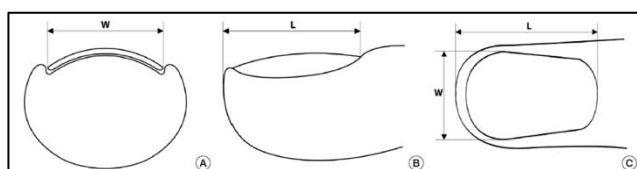


Fig.2 A. An end view of the fingernail, where the width (W) is defined as the farthest transverse distance between two nail points in the lateral groove.

B. Lateral view of the fingernail, where the length (L) is defined as the furthest distance that can be measured between the tip of the finger and the groove resulting from the intersection of the nail fold.

C. The dorsal view of the fingernail

To study the effect of nail plate growth on the measurements, the data were divided into three main groups, where we applied the same acquisition process to the three groups. The first set (G1) consists of photos of volunteer nails from the first acquisition day. At the same time, the second group (G2) was composed of pictures of volunteer nails taken seven days after the initial acquisition. This group consisted of thirty individuals who were part of the first group (G1). The third group (G3) contained twenty-five images taken from the same volunteers in the second group (G2), but sixty days after the initial acquisition. Tables 1 and 2 illustrate the fingernail configurations for the investigated samples and the W/L (width to length) ratio with the radius of transverse fingernail curvature for the age groups under investigation.

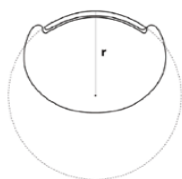


Fig.3 The radius of the circle drawn around the nail whose curve approximates the nail plate

Table 1 thumb fingernail configurations for the investigated samples

Characteristic	Men	Women
Age (year)	45.8±14.2	45.3±13.8
Fingernail width (mm)	14.8±1.0	12.9±1.1
Fingernail length (mm)	14.2±1.0	14.1±1.1
Fingernail W/L ratio	1.02±0.08	0.87±0.08
The transverse fingernail curvature radius (mm)	11.2±1.3	9.4±0.8

HSV COLOR SPACE

One of the RGB color space transformations mainly used in image processes is the Hue Saturation Value (HSV) color space, which is also called the Hue Saturation Brightness (HSB). this technique offers the property of color numerical where Hue illustrates the tint of the color, the saturation shows the shade, and the value describes the luminance. Hue characterizes the most basic colors like Red, Green, and Blue, beside the secondary colors like Magenta, Yellow, and Cyan, as explained in Fig4.

Equations (1), (2), and (3) illustrate the conversion rules to get the (H, S, V) values from RGB color space [18].

$$H = \begin{cases} \left(\frac{G-B}{Max-Min}\right) / 6 & \text{if } R = Max. \\ \left(2 + \frac{B-R}{Max-Min}\right) / 6 & \text{if } G = Max. \\ \left(4 + \frac{B-R}{Max-Min}\right) / 6 & \text{if } B = Max. \end{cases} \dots\dots\dots(1)$$

$$S = \left(\frac{Max}{Max-Min}\right) \dots\dots\dots(2)$$

$$V = Max. \dots\dots\dots(3)$$

Where:

- R: the Red values
- B: the Blue values
- G: the Green values

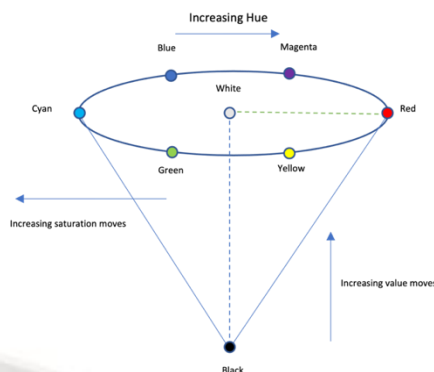


Fig4. HVS color space

GAUSSIAN-BASED FILTER IMAGE SMOOTHING

Blurring is utilized as preprocessing step, as for eliminating the small details that appear on the image earlier to object extraction and aqueduct the small gaps in lines and curves. as follows [19]:

$$f(x, y) = \frac{1}{2\pi\sigma^2} \exp\left(-\frac{x^2+y^2}{2\sigma^2}\right) \dots\dots\dots(4)$$

The smoothing degree depends on the amount of the Gaussian form sigma [20,21].

GRAY SCALE IMAGE CONVERSION

To calculate the gray value from the red, green, and blue colors, one of the following equations was used [20]:

$$f(x, y) = 0.3R + 0.59G + 0.11B \dots\dots\dots(5)$$

$$f(x, Y) = \frac{1}{3}(R + G + B) \dots\dots\dots(6)$$

$$f(x, y) = Threshold\left(\frac{R}{255} + \frac{G}{255} + \frac{B}{255}\right) \dots\dots\dots(7)$$

Where:

- R= Red,
- G= Green, and
- B= Blue

F (x, y) is the corresponding gray value.

ENHANCEMENT OF THE CONTRAST

The analysis of the specific interval was done by determining the minimal and maximal intensity threshold values [21], then the intensity range was stretched to the full range [0-255]. The following linear mapping function was used to calculate the new pixel's brightness values:

$$Img(x, y) = round\left(\frac{(Img(x,y)-Min)}{(Max-Min)}\right) \alpha \times 255 \dots\dots\dots(8)$$

- Min: the minimum value of the intensity for the input image
- Max: the maximum value of the intensity for the input image
- α: the sigma value within the range [21].

THE DETECTION OF THE CANNY EDGE

The major purpose of using the edge detection filter was to reduce the object's amount of data of the used image while protecting that object's essential structure to be used for further analysis.

Canny edge detection became one of the traditional edge detection methods, its algorithm handles in four separate steps [21]: 1. Smoothing the image (Gaussian filter was used for this objective). 2. Computing the intensity gradient of the image (using 2 convolution masks in X and Y directions and finding the gradient). 3. A non-maximum suppression, meaning only labeling the pixels assumed to be part of an edge. 4. Hysteresis, which means selecting the minimum and maximum thresholds and receiving the pixel gradient between these two thresholds.

$$G_x = \begin{bmatrix} -1 & 0 & +1 \\ -2 & 0 & +2 \\ -3 & 0 & +1 \end{bmatrix}$$

$$G_y = \begin{bmatrix} -1 & -2 & -1 \\ 0 & 0 & 0 \\ +1 & +2 & +1 \end{bmatrix} \dots\dots\dots(9)$$

$$G = \sqrt{G_x^2 + G_y^2} \dots\dots\dots(10)$$

III. RESULTS

THE SUGGESTED SYSTEM

The main vision in our approach for fingernail detection is based on using HSV color space, contrast enhancement for

grayscale, and a canny algorithm. Every phase in the suggested detection algorithm was demonstrated with the results. Fig. 5 shows every phase of the suggested system.

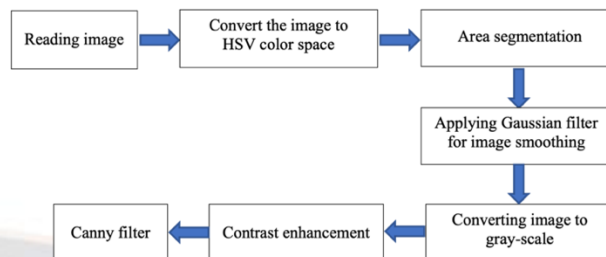


Fig5. Detection algorithm for fingernail image

IMAGE READING

Initially, the color image of the fingernail was provided to the system as a BMP file, the resolution of the color of the image was captured at an amount of 24 bits/pixel. firstly, the image header information was read, for the second stage the pixel data was read, then the values of the red, green, and blue bands were loaded and placed in a 3D matrix with the log. As in table 3.

Table 3 Example of 3D array contents

No. of pixels	Row/Column (x,y)	Z (Preprocessing on x and y)							
		Value			HSV			Skin HSV	Contrast
		Red	Green	Blue	H	S	V		
1	1,1								
	1,2								
	...								
2	2,1								
	2,2								
	...								

X: row pixel image, (0 to Image Width-1)
 Y: column pixel image, (0 to Image High -1)
 Z: containing the values of three bands also all preprocessing on x and y.

HSV COLOR SPACE

In the RGB color space, a very large change in the values of color may not be noticed by the naked eye. so, this color space is not appropriate for fingernail detection, for that, an appropriate space for HSV color was applied to represent the nail color and surrounding space color changes as mentioned earlier, in the suggested system. The aim of this step was to define the fingernail area in the thumb image by first transforming RGB to HSV color space and using particular rules to define the skin area.

FINGER NAIL IMAGE SMOOTHING STEP

After the nail detection stage, image smoothing was the first stage in edge detection to lessen the existing noise and improve the shape of fingernail details by using the Gaussian filter. The sigma with the value of (0.8) and kernel size (3x3) was selected in the suggested system. Figure 6 illustrates the steps used for image processing steps.

Table 4 Color space and channel statistics

	avg	med	min	max
GHB:R	183	220	28	246
RGB:G	145	171	13	226
RGB:B	128	150	7	215
HSV:H	19	1.00	18	4
HSV:S	32	28	10	78
HSV:V	72	86	11	96
LCH:L	62	74	5	91
LCH:C	19	18	7	47
LCH:H	52	1.00	49	27
LAB:L	62	74	5	91
LAB:A	12	12	-4	35
LAB:B	14	14	4	33

CONTRAST ENHANCEMENT

One of the most essential steps in this part is the Contrast enhancement. This technique gives more details about the fingernail which is suitable for this stage of the work. For that, stretching for the contrast was proposed for the gray values.

This procedure was accomplished by using two stages: one is specifying the minimum and the maximum values of the threshold, and second, a linear stretching was applied, in this stage, the low-intensity values which are less than the determined minimum value toward 0, and the high-level values higher than maximum value are moved toward 255. All values which lie between min and max values are linearly mapped by using equation 7. As a result, for that, intensity levels were stretched to the full range between 0 and 255.

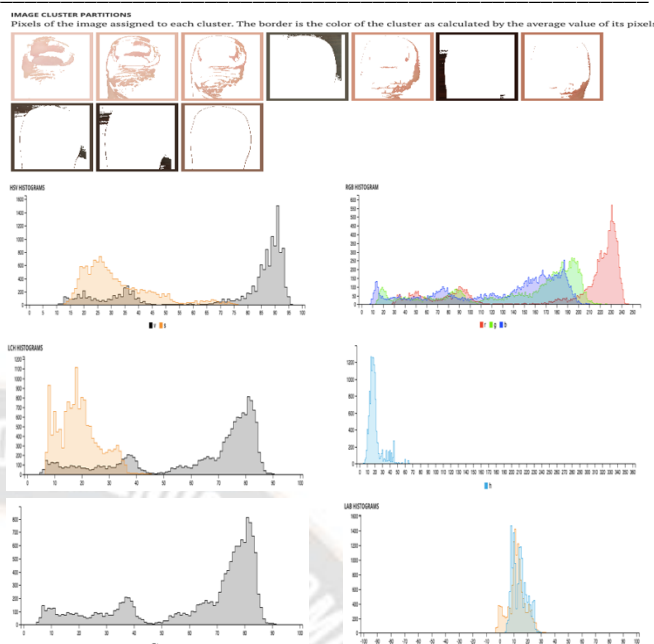


Fig6. Finger nail image processing steps

THE DETECTION OF SUB-STAGE BY USING CANNY EDGE

Edge detection was used to reduce the amount of the in the image, and protect the main structure at the same time to be used for additional processing. Fig 7 illustrates the procedure for applying the Canny filter after image smoothing steps and the grayscale converting steps, where the threshold minimum and maximum values are T=100, and T=20 respectively.

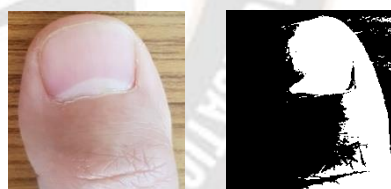


Fig7. Applying Canny Edge filter on the image

DATA SET

The proposed system applied to the Dataset consists of 100 images for the right thumb fingernail taken from donors who were between 20-75 years old both sexes. all images are read as BMP 24 bit/pixel (bit depth). note that all photos were taken from an equal distance under the same illumination conditions to avoid distortion and to get the exact circumstances for each photo under investigation. Figure 8 shows some of the collected photos for the investigation with the sex and age for each volunteer.



Fig8. Examples of the right thumb fingernail used

IV. DISCUSSION

The topic of nail-based biometric authentication is a recent topic, and for this reason, there are not a large number of literature reviews on this topic. Nevertheless, we tried in this article to handle the most relevant topics.

After we divided the groups and studied the effect of the time factor on the growth of the biological change of the nail, the results showed that nail plate growth did not affect the measurements taken or the validation mechanism, so we used nail bed information for ROI. In men, the mean age was 45.8 ± 14.2 years, while in women, the mean age was 45.3 ± 13.8 years. From the results observed, the length and width of the nail, the ratio of length to width, and the half diameter of the curvature of the nail were more considerable in males than it is in females. All these parameters had the most effective value in the thumb of both sexes, and the most significant value of the radius of curvature of the nails in the thumb was obtained for all cases studied and for both sexes.

Through the results obtained from all participants in the test, we found that the change in human age does not affect the ratio of nail length to width W/L, nor does it affect the nail bed. What should be noted is that the higher the person's age, the lower the radius of the nail curvature, meaning that the nails tend to flatten out as the person ages. This information was collected for statistical purposes only and in order to know the effect of age on the variables used in this research.

The essential aim of enhancement of the contrast was to undertake the process for a given image so that the output is suitable for the next step. If any number of picture elements tacking fixed place, that means the image has inferior contrast.

By making a modification to the histogram, every pixel will be modified to a new value that is increasingly populating the range of brightness levels. The Stretching of the Contrast is an image enhancement technique that improves the occupying range of brightness levels. The paramount idea of contrast stretching is to extend the distribution of brightness value to populate all the histogram ranges.

V. CONCLUSIONS

In this project, we have introduced a model to detect and extract fingernail skin using color images by utilizing the HSV color space, which provided better differentiation between the fingernail skin and non-skin ranges. The segmentation of the fingernail skin area was achieved by using a specific range of directions emanating from the HSV color space. The experimental procedure results showed that the proposed technique for modeling the fingernail skin color achieved an excellent accuracy rate and could separate the fingernail skin ranges from the background. Furthermore, the proposed system was applied to a dataset of 100 images for the right thumb, which was read as BMP 24 bit/pixel. The use of Canny edge detection resulted in more precise outcomes due to the utilization of controlled parameter values such as Kernel size of Gaussian Filter = 3×3 , Sigma = 0.8, grayscale threshold = 127, and maximum and minimum thresholds of the canny filter = 100 and 20, respectively.

REFERENCES

- [1] E. A. Abed et al., "Intelligent multimodal identification system based on local feature fusion between iris and finger

- vein," Indonesian Journal of Electrical Engineering and Computer Science, vol. 21, no. 1, pp. 224-232, 2021, <https://doi:10.11591/ijeecs.v21.i1.pp224-232>.
- [2] M. El Beqqal et al., "Multimodal access control system combining RFID, fingerprint and facial recognition," Indonesian Journal of Electrical Engineering and Computer Science, vol. 20, no. 1, pp. 405-413, 2020, <https://doi:10.11591/ijeecs.v20.i1.pp405-413>.
- [3] E. M. Cherrat et al., "A multimodal biometric identification system based on cascade advanced of fingerprint, finger vein and face images," Indonesian Journal of Electrical Engineering and Computer Science, vol. 17, no. 3, pp. 1562-1570, 2020, <https://doi:10.11591/ijeecs.v18.i1.pp1562-1570>.
- [4] E. Haneke, "Anatomy of the nail unit and the nail biopsy," Seminars in Cutaneous Medicine and Surgery, vol. 34, no. 2, pp. 95-100, 2015, <https://doi:10.12788/j.sder.2015.0143>.
- [5] S. Phadke, "The Importance of a Biometric Authentication System," The SIJ Transactions on Computer Science Engineering & Its Applications (CSEA), vol. 01, no. 04, pp. 18-22, 2013, <https://doi:10.9756/sijcsea/v1i4/0104550402>.
- [6] P. R. Cohen, "The lunula," Journal of the American Academy of Dermatology, vol. 34, no. 6, pp. 943-953, 1996, [https://doi:10.1016/S0190-9622\(96\)90269-8](https://doi:10.1016/S0190-9622(96)90269-8).
- [7] M. Arafat Abdel-Maksoud, "Nail-Fold Excision Without Mastoideotomy for Treatment of Ingrown Toe Nails," Al-Azhar Medical Journal, vol. 47, no. 2, pp. 321-328, 2018, <https://doi:10.12816/0052257>.
- [8] I. Reilly, "Nail plate and nail bed trauma," Podium Nail Academy, Summer (12/12), pp. 1-3, 2006.
- [9] B. M. Piraccini, "Nail Anatomy and Physiology for the Clinician," in Nail Disorders, Milano: Springer, 2014, https://doi:10.1007/978-88-470-5304-5_1.
- [10] L. Farran et al., "The effect of humidity on the fracture properties of human fingernails," Journal of Experimental Biology, vol. 211, no. 23, pp. 3677-3681, 2008, <https://doi:10.1242/jeb.023218>.
- [11] L. Farren et al., "The fracture properties and mechanical design of human fingernails," Journal of Experimental Biology, vol. 207, no. 5, pp. 735-741, 2004, <https://doi:10.1242/jeb.00814>.
- [12] M. Barbosa et al., "Secure biometric authentication with improved accuracy," Lecture Notes in Computer Science, vol. 5107 LNCS, pp. 21-36, 2008, https://doi:10.1007/978-3-540-70500-0_3.
- [13] S. Garg et al., "Biometric authentication using finger nail surface," in International Conference on Intelligent Systems Design and Applications, ISDA, 2012, pp. 497-502, <https://doi:10.1109/ISDA.2012.6416588>.
- [14] M. Ong et al., "Touch-less palm print biometrics: Novel design and implementation," Image and Vision Computing, vol. 26, no. 12, pp. 1551-1560, 2008, <https://doi:10.1016/j.imavis.2008.06.010>.
- [15] K. Kale et al., "Multimodal biometric system using fingernail and finger knuckle," in International Symposium on Computational and Business Intelligence, ISCBI, 2013, pp. 279-283, <https://doi:10.1109/ISCBI.2013.63>.
- [16] J. Jung et al., "Fingernail configuration," Archives of Plastic Surgery, vol. 42, no. 6, pp. 753-760, 2015, <https://doi:10.5999/aps.2015.42.6.753>.
- [17] A. O. George, "Finger nail plate shape and size for personal identification--a possible low technology method for the developing world--preliminary report," African Journal of Health Sciences, vol. 12, no. 1-2, pp. 13-20, 2005, <https://doi:10.4314/ajhs.v12i1.30795>.
- [18] J. H. Al-A'meri and S. M. Saber, "Face Detection Based on Robust Algorithm of Skin Color," International Journal of Scientific & Engineering Research, vol. 7, no. 5, pp. 2016, available online: <http://www.ijser.org>.
- [19] C. Solomon and T. Breckon, "Fundamentals of Digital Image Processing (A Practical Approach with Examples in MATLAB)," 1st Edition, Wiley-Blackwell, 2011.
- [20] R. C. Gonzalez and R. E. Woods, "Digital Image Processing," 3rd Edition, Pearson International Edition, 2002.
- [21] A. Hema et al., "A Survey on Feature Extraction Technique in Image Processing," International Journal of Trend in Scientific Research and Development, vol. 2, issue 4, pp. 448-451, 2018.